

https://doi.org/10.1130/G51777.1

Manuscript received 5 October 2023 Revised manuscript received 9 January 2024 Manuscript accepted 24 January 2024

Published online 6 February 2024

© 2024 The Authors. Gold Open Access: This paper is published under the terms of the CC-BY license.

## Precambrian to Pleistocene <sup>40</sup>Ar/<sup>39</sup>Ar dating of clinopyroxenehosted melt inclusions

Brian R. Jicha<sup>1,\*</sup>, Allen J. Schaen<sup>2</sup>, Bryan Wathen<sup>1</sup>, and William O. Nachlas<sup>1</sup>
<sup>1</sup>Department of Geoscience, University of Wisconsin–Madison, Madison, Wisconsin 53706, USA
<sup>2</sup>Department of Geosciences, University of Arizona, Tucson, Arizona 85721, USA

#### **ABSTRACT**

Clinopyroxene is a rock-forming mineral that commonly hosts melt inclusions in mafic to intermediate composition volcanic and plutonic rocks. It is highly resistant to alteration compared to other co-existing phenocrysts such as plagioclase. Several recent studies have <sup>40</sup>Ar/<sup>39</sup>Ar dated clinopyroxene in Neoproterozoic to Miocene basalts and dolerites. To assess the viability of the technique at the youngest end of the geologic time scale, we performed <sup>40</sup>Ar/<sup>39</sup>Ar incremental heating experiments on clinopyroxene-hosted melt inclusions from a variety of mafic lithologies and tectonic settings. Most samples produced precise plateau ages including several Quaternary basalts to andesites as young as 0.6 Ma. All data are indistinguishable from new and/or published 40Ar/39Ar ages on groundmass or plagioclase from the same samples. The source of potassium (K) and resulting 40Ar\* within clinopyroxene has been debated, but thus far has only been inferred based on 40Ar/39Ar data. Using electron probe microanalysis (EPMA) we show that there is negligible K in the clinopyroxene host, but substantial K (e.g., 1-4 wt%) in trapped melt inclusions and minor amounts in plagioclase inclusions. Thus, melt inclusions, which are common in phenocrysts in basaltic magmas, can be used to obtain accurate and precise 40Ar/39Ar ages for difficult-to-date volcanic and plutonic rocks from the Precambrian to the Pleistocene.

### INTRODUCTION

More than half of Earth's surface is covered by mafic oceanic crust and other mafic terranes (ophiolites, flood basalts, exposed arc crust). Precise geochronologic constraints for mafic to ultramafic magmatic systems are often limited due to a lack of U-Th-Pb-bearing minerals (e.g., zircon, baddeleyite, rutile, titanite; Scoates et al., 2021) or a lack of fresh plagioclase, which often alters to sericite yielding <sup>40</sup>Ar/<sup>39</sup>Ar ages associated with the time of hydrothermal alteration (Verati and Jourdan, 2014; Jiang et al., 2021).

Clinopyroxene, on the other hand, is found in mafic volcanic and plutonic rocks from many terrestrial settings (ocean islands, volcanic arcs, intraplate regions, etc.). It is often utilized in igneous petrology as a thermometer (e.g., Lindsley and Andersen, 1983), a hygrometer (Wade et al., 2008), a barometer (e.g., Putirka, 1999, 2008), a recorder of magma ascent rates (Lloyd

Brian R. Jicha https://orcid.org/0000-0002

et al., 2016; Ubide et al., 2019), and for cosmogenic (<sup>3</sup>He and <sup>10</sup>Be) exposure age chronology (e.g., Craig and Poreda, 1986; Balter-Kennedy et al., 2023). Traditionally, clinopyroxene has not been a preferred mineral for <sup>40</sup>Ar/<sup>39</sup>Ar dating due to its extremely low potassium content and high calcium content, the latter of which results in very large <sup>37</sup>Ar signals that can be implanted in the mass spectrometer causing analytical noise.

<sup>40</sup>Ar/<sup>39</sup>Ar age determinations had previously only been obtained on very old clinopyroxene in chondrites and/or achondrites (e.g., Kennedy et al., 2013), eclogites (e.g., Wang et al., 2000), or as inclusions in diamonds from kimberlites (Phillips et al., 1989, 2004; Burgess et al., 2004). However, three recent studies (Ware and Jourdan, 2018; Konrad et al., 2019; Zi et al., 2019) have shown that Neoproterozoic to Miocene clinopyroxene phenocrysts can now be precisely <sup>40</sup>Ar/<sup>39</sup>Ar dated due to the improved collector/amplifier technology in multi-collector noble gas mass spectrometers (e.g., Cox et al., 2020).

The source of K and radiogenic daughter product (40Ar\*) in clinopyroxene has been unclear. Ware and Jourdan (2018) compared the signal intensities during analyses of pyroxene and plagioclase from the same sample and conducted numerical modeling to suggest that pure pyroxene was dated. Conversely, Konrad et al. (2019) interpreted the K/Ca spectra to reflect the presence of a high-K phase within the clinopyroxene, such as nanoscale silicate mineral inclusions along grain defects or secondary melt inclusion bands. However, neither of these studies attempted to quantify the source(s) of K within the clinopyroxene.

We used scanning electron microscope (SEM) imaging and energy-dispersive X-ray spectroscopy (EDS) to characterize the identity and distribution of mineral inclusions in clinopyroxene, along with electron probe microanalysis (EPMA) to quantify the sources of K and subsequent <sup>40</sup>Ar\* within clinopyroxene. This characterization approach facilitates the use of clinopyroxene-hosted K-rich melt inclusions, which produce precise <sup>40</sup>Ar/<sup>39</sup>Ar ages for mafic rocks spanning most of the geologic time scale that otherwise may not be dated with other geochronologic techniques.

#### **METHODS**

## Sample Selection and Characterization of Clinopyroxene and Inclusions

The analyzed clinopyroxenes came from 11 mafic samples (10 volcanic, 1 plutonic) from the Aleutian arc (Powers et al., 1960; Jicha et al., 2006, 2012; Schaen et al., 2016; Coombs and Jicha, 2021), the Central American arc (Jicha and Hernández, 2022), and from seamounts fed by the Hawaiian mantle plume (Jicha et al., 2018). Most samples were chosen because there are published <sup>40</sup>Ar/<sup>39</sup>Ar age constraints from other K-bearing phases such as plagioclase or groundmass. None of the clinopyroxene crystals

CITATION: Jicha, B.R., et al., 2024, Precambrian to Pleistocene <sup>40</sup>Ar/<sup>39</sup>Ar dating of clinopyroxene-hosted melt inclusions: Geology, v. 52, p. 287–291, https://doi.org/10.1130/G51777.1

<sup>\*</sup>brian.jicha@wisc.edu

showed evidence of alteration or exsolution under a binocular microscope or SEM at the millimeter to micrometer scale.

Clinopyroxene crystals were mounted in 2.5-cm-diameter round epoxy mounts, ground to the interior of the crystals, polished, and coated with 20 nm of carbon. A Hitachi S-3400N Type-II Variable Pressure SEM was used under high vacuum at <1 Pa with a 15 kV accelerating voltage and 10 mm working distance to investigate each clinopyroxene crystal and its inclusions. Because plagioclase and melt inclusions have similar backscattered electron contrast, EDS spectra were used to identify and qualitatively assess the compositions of the inclusions.

A Cameca SX-Five FE-EPMA was used to (1) quantify the trace K concentration in the host clinopyroxene, and (2) measure the major and minor element content of mineral and melt inclusions. Details of the EPMA methodology, including analysis conditions, primary standards, and evaluation of reference materials, are provided in the Supplemental Material.<sup>1</sup>

## 40Ar/39Ar Methods

Clinopyroxene (150–1500  $\mu m$ ) was ultrasonically leached in 3 M HCl for 10 min, rinsed repeatedly with deionized water, and then hand-picked under a binocular microscope. The purified separates were irradiated in the cadmium-lined in-core tube at the Oregon State University (Corvallis, USA) reactor. The 1.1864 Ma Alder Creek sanidine (Jicha et al., 2016) or the 28.201 Ma Fish Canyon sanidine (Kuiper et al., 2008) were used as a neutron fluence monitor for 2–50 h irradiations.

<sup>1</sup>Supplemental Material. <sup>40</sup>Ar/<sup>39</sup>Ar data tables and diagrams. Please visit https://doi.org/10.1130/GEOL .S.25057754 to access the supplemental material; contact editing@geosociety.org with any questions.

<sup>40</sup>Ar/<sup>39</sup>Ar analyses were conducted in the WiscAr Geochronology Laboratory at the University of Wisconsin-Madison (USA). Clinopyroxene aliquots (12-37 mg) were placed in a 5-mm-diameter well in a copper tray and incrementally heated with a 55 W CO<sub>2</sub> laser. The gas released during each heating step was cleaned with two SAES GP50 getters (50 W, 400 °C) and an ARS cryotrap (at -125 °C). Isotopic analyses were done using an Isotopx NGX-600 mass spectrometer (Mixon et al., 2022). Because it is critical to assess any subtle changes in instrument and/or background conditions during analyses of these challenging, low-K samples, we measured a blank and an aliquot of air before and after every sample heating step for calibration. All of the 40Ar/39Ar ages are calculated using the decay constants of Min et al. (2000) and are reported with  $2\sigma$  analytical uncertainties, including the J uncertainty (e.g., Schaen et al., 2020; see the Supplemental Material).

### RESULTS

## **Clinopyroxene and Inclusion Compositions**

Transects consisting of six EPMA analyses were performed across the long axis of ten clinopyroxene crystals in each sample (i.e., 60 analyses/sample). All of the clinopyroxene are augite or titano-augite (Table 1), and none were chemically zoned. All analyzed clinopyroxene crystals yielded K concentrations below the detection limit (6 ppm).

Small inclusions (plagioclase, ilmenite, magnetite, apatite, and trapped melt), which range from  $<5 \,\mu m$  to  $40 \,\mu m$  in diameter, were observed in the clinopyroxene in the seven samples we analyzed (Fig. 1; see the Supplemental Material). Clinopyroxene in samples 90T072B and 14AKMC064 were inclusion-free or contained very few inclusions (1–6 per polished crystal surface). In contrast, samples 72-20-AA and ES-13-

03 contained abundant small inclusions (ilmenite/magnetite > plagioclase > melt) (Fig. 1).

Most melt inclusions have andesitic to dacitic major element compositions (Table 1; Fig. 1), whereas those from two samples (ES-13-03, TAN-07-21) are rhyolitic, one of which has an average of 3.5 wt%  $K_2O$ . The major element compositions of the plagioclase inclusions are generally similar (Table 1). The  $K_2O$  contents of individual plagioclase inclusions range from 0.04 to 0.90 wt%, with an average plagioclase  $K_2O$  content of 0.3–0.6 wt% per sample.

## <sup>40</sup>Ar/<sup>39</sup>Ar Incremental Heating

Incremental heating experiments from 9 of 11 samples produced 40Ar/39Ar plateau ages ranging from  $30.73 \pm 0.46$  Ma to  $0.62 \pm 0.04$  Ma (Fig. 2; see the Supplemental Material). Because all of the isochrons have intercepts that are within uncertainty of the atmospheric value (Fig. 2), the plateau ages are preferred. Experiments on two samples, a 253 ka basalt (TAN-07-21) and a 365 ka basaltic andesite (14AKMC064), yielded negligible amounts of radiogenic Ar, and thus no age information could be obtained from the clinopyroxene in these very young samples. Because four of the rocks from which we dated clinopyroxene-hosted melt inclusions did not have any published age information, we also performed incremental heating experiments on groundmass or plagioclase from these samples. The ages from these phases are indistinguishable from the clinopyroxene ages in the same sample (Fig. 2; see the Supplemental Material).

### DISCUSSION

## <sup>40</sup>Ar/<sup>39</sup>Ar Dating of Clinopyroxene-Hosted Melt Inclusions from the Pleistocene to the Precambrian

Prior to our work, the youngest clinopyroxene 40Ar/39Ar age that has been corrobo-

TADLE 4 A	AVED A OF COMPOSITIONS	OF OUNODVDOVENE CAMPI	EC AND THEIR INCLUDIONO (1.40/)	`
TABLE I. F	AVERAGE COMPOSITIONS	OF CLINOPYROXENE SAMPL	.ES AND THEIR INCLUSIONS (wt%)	)

Sample	Host cpx/ inclusion		SiO <sub>2</sub>	TiO <sub>2</sub>	Al <sub>2</sub> O <sub>3</sub>	FeO	MnO	MgO	CaO	Na <sub>2</sub> O	K₂O	Cr <sub>2</sub> O <sub>3</sub>	Total
12AKMC028	срх	n = 60	49.86	0.64	3.98	8.72	0.28	15.23	20.50	0.37	_	0.05	99.62
	plag inc.	n = 9	54.04	0.07	28.20	1.24	0.02	0.12	11.26	4.85	0.31	_	100.10
	melt inc.	n = 25	64.60	0.42	19.76	1.92	0.09	0.27	3.03	6.19	2.04	_	98.31
14AKMC064	срх	n = 60	50.31	0.58	3.51	9.60	0.38	15.17	19.83	0.37	-	0.00	99.76
	plag inc.	n = 11	51.86	0.03	30.35	0.92	0.02	0.05	13.08	3.91	0.19	_	100.41
	melt inc.	n = 4	58.72	0.19	20.65	2.07	0.07	1.94	8.09	6.64	0.81	_	99.17
OGL-13-02	срх	n = 60	47.82	0.88	7.01	7.62	0.16	14.08	21.78	0.39	_	0.07	99.81
	plag inc.	n = 4	53.21	0.10	28.45	1.33	0.01	0.17	12.10	4.51	0.39	_	100.29
	melt inc.	n = 9	60.25	1.01	20.65	2.69	0.10	1.10	4.82	4.80	1.11	_	96.54
90T072B	срх	n = 60	48.48	1.84	5.03	6.95	0.12	14.76	21.73	0.45	-	0.40	99.76
	melt inc.	n = 9	64.39	0.47	20.84	0.87	0.07	0.40	1.86	6.57	2.34	_	97.81
ES-13-03	срх	n = 60	51.70	0.31	1.26	10.31	0.60	14.50	20.58	0.37	-	0.00	99.63
	plag inc.	n = 10	57.66	0.02	26.75	0.63	0.01	0.04	8.98	6.04	0.64	_	100.76
	melt inc.	n = 20	75.13	0.14	14.05	0.44	0.03	0.02	0.47	4.01	3.55	_	97.85
72-20-AA	срх	n = 60	48.89	2.10	3.99	8.59	0.17	14.16	21.20	0.54	-	0.01	99.66
	plag inc.	n = 16	55.07	0.21	28.07	0.83	0.01	0.09	10.31	5.30	0.48	_	100.38
	melt inc.	n = 7	62.60	0.30	22.09	0.80	0.02	0.31	1.28	8.90	2.25	_	98.55
TAN-07-21	срх	n = 60	47.60	0.91	7.11	7.11	0.13	13.95	22.73	0.31	_	0.09	99.95
	plag inc.	n = 18	51.86	0.07	30.62	0.98	0.01	0.07	13.42	3.69	0.28	_	101.01
	melt inc.	n = 5	70.03	0.13	18.14	0.33	0.03	0.20	1.82	6.35	1.43	-	98.47

Note: cpx—clinopyroxene; plag—plagioclase; inc.—inclusion. Dashes represent below detection limit. Average clinopyroxene compositions are based on six analyses per crystal in 10 crystals per sample. All clinopyroxene analyses had potassium contents that were below the detection limit of 6 ppm (0.0006 wt%).

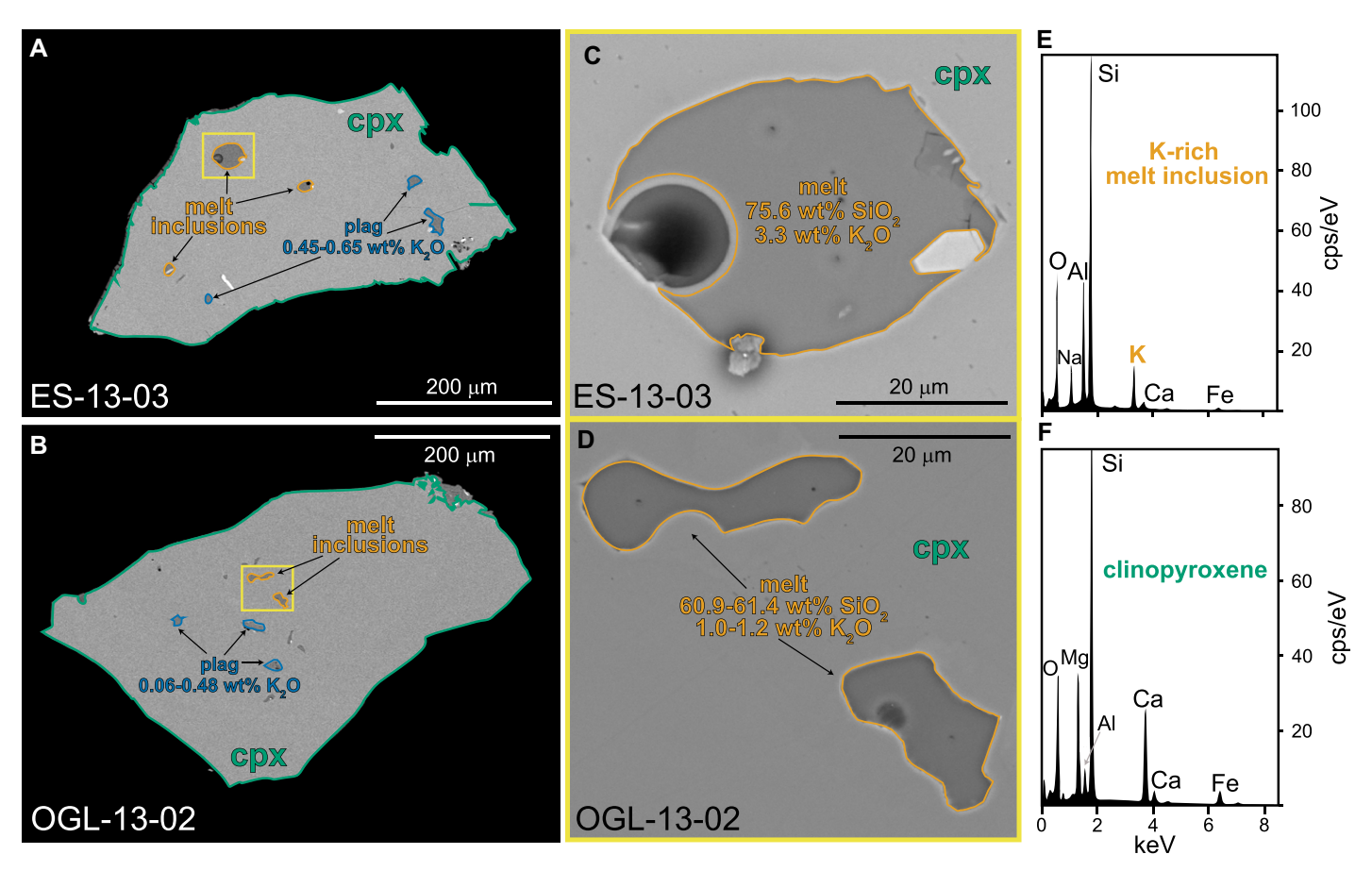


Figure 1. (A, B) Backscattered electron images of clinopyroxene (cpx; green outline) and melt (orange outlines) and plagioclase (plag; blue outlines) inclusions. (C, D) Melt inclusions can be as large as 40  $\mu$ m, occasionally contain vapor bubbles, and have andesitic to rhyolitic compositions with up to 3.5 wt%  $K_2O$ . (E) Energy-dispersive X-ray spectroscopy (EDS) spectra of a typical melt inclusion. (F) EDS spectra of a host clinopyroxene. All quantitative data are from electron probe microanalysis (EPMA) analyses; EDS spectra are shown for qualitative element identification.

rated by data from another co-existing phase is  $47.4 \pm 2.9$  Ma (Konrad et al., 2019). However, Konrad et al. (2019) obtained clinopyroxene ages as young as  $11.5 \pm 1.0$  Ma, which agree with the volcanic stratigraphy. Our 40Ar/39Ar data from both clinopyroxene and groundmass or plagioclase within the same sample demonstrate that clinopyroxene-hosted melt inclusions can be used to obtain 40Ar/39Ar ages as young as 0.6 Ma (Fig. 3). The <0.6 Ma samples that failed to yield sufficient 40Ar\* had very few trapped melt inclusions (see the Supplemental Material). Our results, coupled with previously published 40Ar/39Ar data (Ware and Jourdan, 2018; Konrad et al., 2019; Zi et al., 2019), indicate that melt inclusions within clinopyroxene can provide precise and accurate 40Ar/39Ar ages for ultramafic to intermediate volcanic and plutonic rocks from the Pleistocene to the Precambrian (Fig. 3).

# Source of K and Radiogenic <sup>40</sup>Ar\* within the Clinopyroxene

The source of K and daughter product <sup>40</sup>Ar\* in clinopyroxene has been a matter of debate. Based on the K/Ca spectrum shape and the high

closure temperature of clinopyroxene (730 °C; Cassata et al., 2011), Konrad et al. (2019) suggested that their <sup>40</sup>Ar/<sup>39</sup>Ar data are likely the result of degassing of a phase trapped within the crystal. Primary melt inclusions were ruled out as they argued that these inclusions could carry the <sup>40</sup>Ar/<sup>36</sup>Ar signature of the mantle, which is several orders of magnitude higher than the that of the atmosphere. Konrad et al. (2019) suggested that either secondary melt inclusion bands or nanoscale silicate inclusions along grain defects and/or cleavage planes are the best candidates to harbor K and <sup>40</sup>Ar\*.

In contrast, Ware and Jourdan (2018) suggested that the distinct "stair step" K/Ca spectrum shape and <sup>39</sup>Ar release pattern throughout their experiments are due to a difference in Ca concentration between the augite (high-Ca pyroxene) and pigeonite (low-Ca pyroxene) within grains. They also noted that plagioclase inclusions, if present, would have to be nanocrystalline in size. Thus, both Konrad et al. (2019) and Ware and Jourdan (2018) invoked the presence of nanosilicate inclusions, which would be volumetrically insignificant and unlikely to produce the <sup>39</sup>Ar significant

nals observed during incremental heating of the clinopyroxene.

In each of the recent studies involving <sup>40</sup>Ar/<sup>39</sup>Ar dating of clinopyroxene, no quantitative chemical analyses of the inclusions or the host clinopyroxene were performed. Our EPMA measurements indicate that there is negligible K in the augite phenocrysts, but substantial K (up to 4 wt%) in trapped primary melt inclusions that range from  $<5 \,\mu m$  to  $40 \,\mu m$  in diameter, and minor amounts of K (average 0.3–0.6 wt% K<sub>2</sub>O) in plagioclase inclusions (Fig. 1). Moreover, the inclusions give isochrons with atmospheric <sup>40</sup>Ar/<sup>36</sup>Ar intercepts, which is in contrast to the suggestion of Konrad et al. (2019) that primary melt inclusions would have mantle-like 40Ar/36Ar ratios. Assuming the primary melt inclusions are the source of the measured 39Ar at low- to mid-temperature heating steps, the atmospheric intercepts also imply that clinopyroxene crystallization and entrapment of primary melt inclusions likely occurred at shallow depths during magma storage and degassing in the upper crust.

To further quantify the K budget in clinopyroxene, we used ImageJ software (https:// imagej.net/software/imagej/; Schneider et al.,

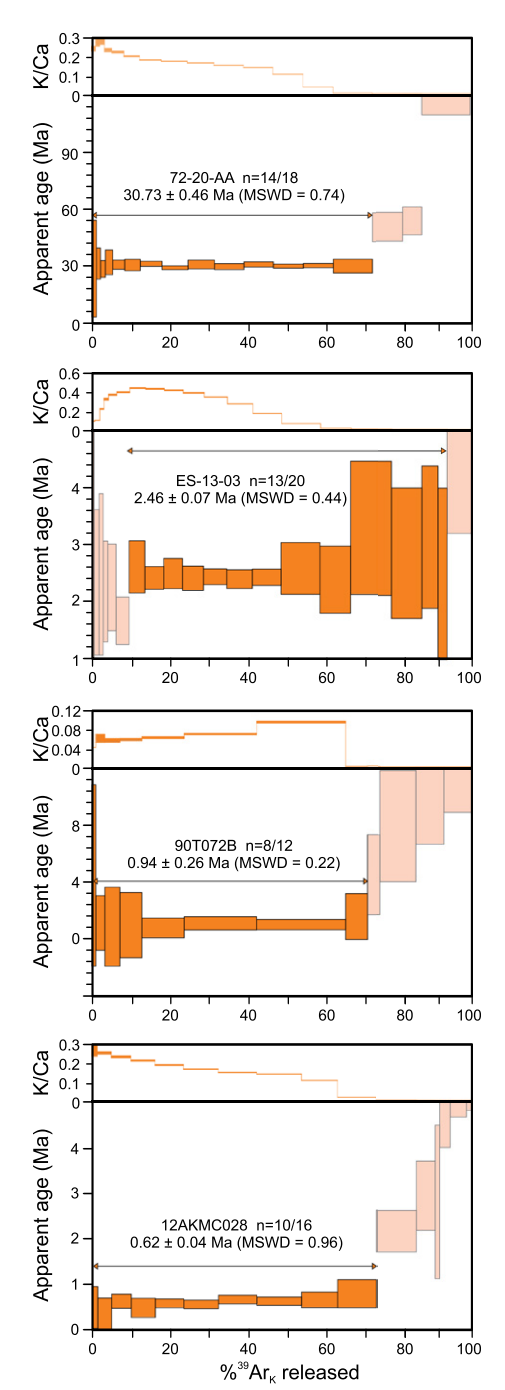


Figure 2. Representative <sup>40</sup>Ar/<sup>39</sup>Ar incremental heating age spectra, K/Ca variation, and inverse isochron diagrams for Oligocene to Quaternary clinopyroxene. Arrows indicate the selected plateau range. All uncertainties are displayed at the 2σ confidence level. MSWD—mean square of weighted deviation.

2012) to estimate the area fraction of K-rich inclusions within 6–10 clinopyroxene crystals from each sample, and they range from  $\sim 2\%$  to >5%. This translates to  $\sim 200$ –500 ppm K within each crystal assuming an average  $K_2O$  content of  $\sim 1$  wt% for the melt + plagioclase inclusions. Therefore, we interpret the different K/Ca spectra patterns in each of our analyses

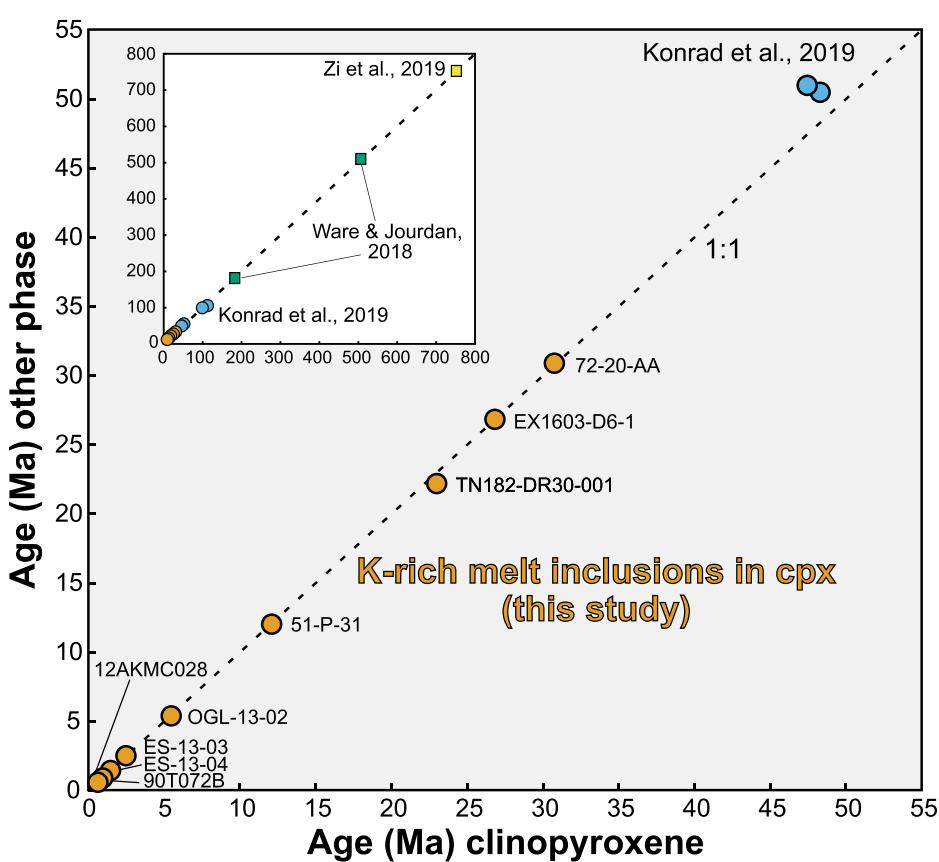


Figure 3. Comparison of <sup>40</sup>Ar/<sup>39</sup>Ar age determinations from clinopyroxene (cpx) and other co-existing phases. A dashed 1:1 line is shown for reference. Age determinations from this study are in orange. Inset is a continuation of the plot to 800 Ma showing the data of Konrad et al. (2019) (blue), Ware and Jourdan (2018) (green), and Zi et al. (2019) (yellow). All data sets show excellent agreement between the clinopyroxene <sup>40</sup>Ar/<sup>39</sup>Ar ages and co-existing phases down to 0.6 Ma.

to be a function of the variable proportions of K-bearing inclusions in each sample combined with the custom laser heating schedules used to degas the samples. The percent 39Ar patterns and shape of the age spectra are generally similar (Fig. 2). The first 50%-70% of the <sup>39</sup>Ar released contains the most precise steps, which is primarily attributed to the degassing of the melt inclusions. Expansion of the melt inclusions upon magma decompression may result in the development of fractures within the host clinopyroxene along the margins of the melt inclusions, which may serve as an initial pathway for gas to escape during laser heating. Larger melt inclusions are more likely to crack their mineral host (Kent, 2008). The high temperature steps often have very large uncertainties and give older ages, and likely reflect degassing of the plagioclase inclusions containing excess Ar or the clinopyroxene itself, both of which are consistent with the large observed <sup>37</sup>Ar signals. These steps cannot be attributed to the presence of another more Ca-rich pyroxene (e.g., Ware and Jourdan, 2018) because we did not observe any exsolution or compositional zoning in our clinopyroxene samples.

## CONCLUSIONS AND FUTURE OPPORTUNITIES

Multi-collector noble gas mass spectrometers with improved collector/amplifier technology are expanding the capabilities of the 40Ar/39Ar chronometer. 40Ar/39Ar incremental heating experiments performed on clinopyroxene-hosted melt inclusions in mafic to intermediate rocks from various tectonic settings produced precise plateau ages, including Quaternary basalts to andesites as young as 0.6 Ma. All data are indistinguishable from new and/or published <sup>40</sup>Ar/<sup>39</sup>Ar ages on co-existing minerals within the same samples. 40Ar/39Ar data from an Aleutian gabbro suggest that clinopyroxene could be a useful high-temperature chronometer in mafic to ultramafic plutonic systems, including those where K-rich phases or zircon are limited or absent (e.g., layered mafic intrusions, ophiolites, lower arc crust). SEM characterization of the clinopyroxene indicates the presence of small inclusions, which range from  $<5 \mu m$  to  $40 \mu m$ in diameter, that vary in abundance and composition. EPMA reveals negligible K in the clinopyroxene host, but substantial K (up to 4 wt%) in trapped melt inclusions and minor amounts in plagioclase inclusions. K-rich melt inclusions within the clinopyroxene enable <sup>40</sup>Ar/<sup>39</sup>Ar geochronology of young mafic rocks that otherwise may not be datable with other techniques. Our results, coupled with the near-ubiquitous presence of melt inclusions in most basaltic magmas (e.g., Kent, 2008), suggest that clinopyroxene and potentially other K-poor mafic phenocrysts (olivine, orthopyroxene) and accessory minerals (e.g., apatite) with trapped melt inclusions, can be used to obtain accurate and precise <sup>40</sup>Ar/<sup>39</sup>Ar ages for volcanic rocks from the Pleistocene to the Precambrian.

#### ACKNOWLEDGMENTS

This research was supported, in part, by U.S. National Science Foundation grants OCE-1834723 and OCE-2135694. We thank Kevin Konrad, Stephen Cox, and Steven Jaret for their very helpful reviews.

## REFERENCES CITED

- Balter-Kennedy, A., et al., 2023, Cosmogenic <sup>10</sup>Be in pyroxene: Laboratory progress, production rate systematics, and application of the <sup>10</sup>Be–<sup>3</sup>He nuclide pair in the Antarctic Dry Valleys: Geochronology, v. 5, p. 301–321, https://doi.org/10.5194/gchron-5-301-2023.
- Burgess, R., Kiviets, G., and Harris, J., 2004, Ar–Ar age determinations of eclogitic clinopyroxene and garnet inclusions in diamonds from the Venetia and Orapa kimberlites: Lithos, v. 77, p. 113–124, https://doi.org/10.1016/j.lithos.2004.03.048.
- Cassata, W.S., Renne, P.R., and Shuster, D.L., 2011, Argon diffusion in pyroxenes: Implications for thermochronometry and mantle degassing: Earth and Planetary Science Letters, v. 304, p. 407–416, https://doi.org/10.1016/j.epsl.2011.02.019.
- Coombs, M.L., and Jicha, B.R., 2021, The eruptive history, magmatic evolution, and influence of glacial ice at long-lived Akutan volcano, eastern Aleutian Islands, Alaska, USA: Geological Society of America Bulletin, v. 133, p. 963–991, https://doi.org/10.1130/B35667.1.
- Cox, S.E., Hemming, S.R., and Tootell, D., 2020, The Isotopx NGX and ATONA Faraday amplifiers: Geochronology, v. 2, p. 231–243, https://doi.org/10.5194/gchron-2-231-2020.
- Craig, H., and Poreda, R.J., 1986, Cosmogenic <sup>3</sup>He in terrestrial rocks: The summit lavas of Maui: Proceedings of the National Academy of Sciences of the United States of America, v. 83, p. 1970–1974, https://doi.org/10.1073/pnas.83.7.1970.
- Jiang, Q., Jourdan, F., Olierook, H.K.H., Merle, R.E., Verati, C., and Mayers, C., 2021, 40Ar/39Ar dating of basaltic rocks and the pitfalls of plagioclase alteration: Geochimica et Cosmochimica Acta, v. 314, p. 334–357, https://doi.org/10.1016/j.gca .2021.08.016.
- Jicha, B.R., and Hernández, W., 2022, Effusive and explosive eruptive history of the Ilopango caldera complex, El Salvador: Journal of Volcanology and Geothermal Research, v. 421, https://doi.org /10.1016/j.jvolgeores.2021.107426.
- Jicha, B.R., Scholl, D.W., Singer, B.S., Yogodzinski, G.M., and Kay, S.M., 2006, Revised age of Aleutian Island Arc formation implies high rate of magma production: Geology, v. 34, p. 661–664, https://doi.org/10.1130/G22433.1.

- Jicha, B.R., Coombs, M.L., Calvert, A.T., and Singer, B.S., 2012, Geology and <sup>40</sup>Arf<sup>39</sup>Ar geochronology of the medium- to high-K Tanaga volcanic cluster, western Aleutians: Geological Society of America Bulletin, v. 124, p. 842–856, https://doi .org/10.1130/B30472.1.
- Jicha, B.R., Singer, B.S., and Sobol, P., 2016, Re-evaluation of the ages of <sup>40</sup>Ar/<sup>39</sup>Ar sanidine standards and supereruptions in the western U.S. using a Noblesse multi-collector mass spectrometer: Chemical Geology, v. 431, p. 54–66, https://doi.org/10.1016/j.chemgeo.2016.03.024.
- Jicha, B.R., Garcia, M.O., and Wessel, P., 2018, Mid-Cenozoic Pacific plate motion change: Implications for the Northwest Hawaiian Ridge and circum-Pacific: Geology, v. 46, no. 11, p. 939–942, https://doi.org/10.1130/G45175.1.
- Kennedy, T., Jourdan, F., Bevan, A.W., Gee, M.M., and Frew, A., 2013, Impact history of the HED parent body(ies) clarified by new <sup>40</sup>Ar/<sup>39</sup>Ar analyses of four HED meteorites and one anomalous basaltic achondrite: Geochimica et Cosmochimica Acta, v. 115, p. 162–182, https://doi.org/10.1016/j.gca.2013.03.040.
- Kent, A.J., 2008, Melt inclusions in basaltic and related volcanic rocks: Reviews in Mineralogy and Geochemistry, v. 69, p. 273–331, https://doi.org /10.2138/rmg.2008.69.8.
- Konrad, K., Koppers, A.A.P., Balbas, A.M., Miggins, D.P., and Heaton, D.E., 2019, Dating clinopyroxene phenocrysts in submarine basalts using <sup>40</sup>Ar/<sup>39</sup>Ar geochronology: Geochemistry, Geophysics, Geosystems, v. 20, p. 1041–1053, https:// doi.org/10.1029/2018GC007697.
- Kuiper, K., Deino, A., Hilgen, F., Krijgsman, W., Renne, P., and Wijbrans, J., 2008, Synchronizing rock clocks of Earth history: Science, v. 320, p. 500–504, https://doi.org/10.1126/science .1154339.
- Lindsley, D.H., and Andersen, D.J., 1983, A twopyroxene thermometer: Journal of Geophysical Research, v. 88, p. A887–A906, https://doi.org /10.1029/JB088iS02p0A887.
- Lloyd, A.S., Ferriss, E., Ruprecht, P., Hauri, E.H., Jicha, B.R., and Plank, T., 2016, An assessment of clinopyroxene as a recorder of magmatic water and magma ascent rate: Journal of Petrology, v. 57, p. 1865–1886, https://doi.org/10.1093/petrology/egw058.
- Min, K., Mundil, R., Renne, P.R., and Ludwig, K.R., 2000, A test for systematic errors in <sup>40</sup>Ar/<sup>39</sup>Ar geochronology through comparison with U/Pb analysis of a 1.1-Ga rhyolite: Geochimica et Cosmochimica Acta, v. 64, p. 73–98, https://doi.org/10.1016/S0016-7037(99)00204-5.
- Mixon, E.E., Jicha, B.R., Tootell, D., and Singer, B.S., 2022, Optimizing <sup>40</sup>Ar/<sup>39</sup>Ar analyses using an Isotopx NGX-600 mass spectrometer: Chemical Geology, v. 593, https://doi.org/10.1016/j.chemgeo.2022.120753.
- Phillips, D., Onstott, T., and Harris, J., 1989, <sup>40</sup>Ar/<sup>39</sup>Ar laser-probe dating of diamond inclusions from the Premier Kimberlite: Nature, v. 340, p. 460–462, https://doi.org/10.1038/340460a0.
- Phillips, D., Harris, J., and Kiviets, G., 2004, <sup>40</sup>Ar/<sup>39</sup>Ar analyses of clinopyroxene inclusions in African diamonds: Implications for source ages of detrital diamonds: Geochimica et Cosmochimica Acta, v. 68, p. 151–165, https://doi.org/10.1016/S0016-7037(03)00411-3.
- Powers, H.A., Coats, R.R., and Nelson, W.H., 1960, Geology and submarine physiography of

- Amchitka Island, Alaska: U.S. Geological Survey Bulletin 1028-P, 40 p., https://pubs.usgs.gov/bul/1028p/report.pdf.
- Putirka, K., 1999, Clinopyroxene + liquid equilibria to 100 kbar and 2450K: Contributions to Mineralogy and Petrology, v. 135, p. 151–163, https://doi.org/10.1007/s004100050503.
- Putirka, K.D., 2008, Thermometers and barometers for volcanic systems: Reviews in Mineralogy and Geochemistry, v. 69, p. 61–120, https://doi.org/10.2138/rmg.2008.69.3.
- Schaen, A.J., Jicha, B.R., Kay, S.M., Singer, B.S., and Tibbetts, A., 2016, Eocene to Pleistocene magmatic evolution of the Delarof Islands, Aleutian Arc: Geochemistry, Geophysics, Geosystems, v. 17, p. 1086–1108, https://doi.org/10.1002 /2015GC006067.
- Schaen, A.J., et al., 2020, Interpreting and reporting <sup>40</sup>Ar/<sup>39</sup>Ar geochronologic data: Geological Society of America Bulletin, v. 133, p. 461–487, https://doi.org/10.1130/B35560.1.
- Schneider, C.A., Rasband, W.S., and Eliceiri, K.W., 2012, NIH Image to ImageJ: 25 years of image analysis: Nature Methods, v. 9, p. 671–675, https://doi.org/10.1038/nmeth.2089.
- Scoates, J.S., Wall, C.J., Friedman, R.M., Weis, D., Mathez, E.A., and VanTongeren, J.A., 2021, Dating the Bushveld Complex: Timing of crystallization, duration of magmatism, and cooling of the world's largest layered intrusion and related rocks: Journal of Petrology, v. 62, https://doi.org/10.1093/petrology/egaa107.
- Ubide, T., Mollo, S., Zhao, J.X., Nazzari, M., and Scarlato, P., 2019, Sector-zoned clinopyroxene as a recorder of magma history, eruption triggers, and ascent rates: Geochimica et Cosmochimica Acta, v. 251, p. 265–283, https://doi.org/10.1016/j.gca.2019.02.021.
- Verati, C., and Jourdan, F., 2014, Modelling effect of sericitization of plagioclase on the <sup>40</sup>K/<sup>40</sup>Ar and <sup>40</sup>Ar/<sup>39</sup>Ar chronometers: Implication for dating basaltic rocks and mineral deposits, *in* Jourdan, F., et al., eds., Advances in <sup>40</sup>Ar/<sup>39</sup>Ar Dating: From Archaeology to Planetary Sciences: Geological Society, London, Special Publication 378, p. 155–174, https://doi.org/10.1144/SP378.14.
- Wade, J.A., Plank, T., Hauri, E.H., Kelley, K.A., Roggensack, K., and Zimmer, M., 2008, Prediction of magmatic water contents via measurement of H<sub>2</sub>O in clinopyroxene phenocrysts: Geology, v. 36, p. 799–802, https://doi.org/10.1130/G24964A.1.
- Wang, S., Ge, N., Sang, H., and Qiu, J., 2000, Genesis of excess argon in phengite and significance of <sup>40</sup>Ar-<sup>39</sup>Ar age spectra for omphacite: A case study on UHP eclogite of South Dabie Terrain, China: Chinese Science Bulletin, v. 45, p. 1345–1351, https://doi.org/10.1007/BF02886233.
- Ware, B., and Jourdan, F., 2018, 40 Ar/39 Ar geochronology of terrestrial pyroxene: Geochimica et Cosmochimica Acta, v. 230, p. 112–136, https://doi.org/10.1016/j.gca.2018.04.002.
- Zi, J.-W., Haines, P.W., Wang, X.-C., Jourdan, F., Rasmussen, B., Halverson, G.P., Sheppard, S., and Li, C.-F., 2019, Pyroxene <sup>40</sup>Ar/<sup>39</sup>Ar dating of basalt and applications to large igneous provinces and Precambrian stratigraphic correlations. Journal of Geophysical Research: Solid Earth, v. 124, p. 8313–8330, https://doi.org/10.1029 /2019JB017713.

Printed in the USA